Cooling rate of chondrules in ordinary chondrites revisited by a new geospeedometer based on the compensation rule

Frédéric Béjina, Violaine Sautter, Olivier Jaoul

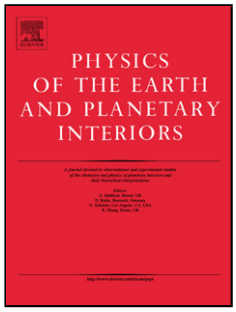

Title: Cooling rate of chondrules in ordinary chondrites revisited by a new geospeedometer based on the compensation rule

Authors: Frédéric Béjina, Violaine Sautter, Olivier Jaoul

PII: S0031-9201(08)00235-5
DOI: doi:10.1016/j.pepi.2008.08.014
Reference: PEPI 5054

To appear in: *Physics of the Earth and Planetary Interiors*

Received date: 5-10-2007
Revised date: 1-8-2008
Accepted date: 18-8-2008

Please cite this article as: Béjina, F., Sautter, V., Jaoul, O., Cooling rate of chondrules in ordinary chondrites revisited by a new geospeedometer based on the compensation rule, *Physics of the Earth and Planetary Interiors* (2007), doi:10.1016/j.pepi.2008.08.014

Cooling rate of chondrules in ordinary chondrites revisited by a new geospeedometer based on the compensation rule

Frédéric Béjina [a,*] Violaine Sautter [b] Olivier Jaoul [a]

[a] *Laboratoire des Mécanismes et Transferts en Géologie, Université de Toulouse - CNRS - IRD - OMP, 14, avenue Édouard Belin, 31400 Toulouse, France*

[b] *Museum National d'Histoire Naturelle, Dept. Histoire de la Terre, 61 rue Buffon, 75005 Paris, France*

Abstract

For several decades efforts to constrain chondrite cooling rates from diffusion zoning in olivine gave rise to a range of values from 5 to 8400 K/hr (Desch and Connolly Jr., 2002; Greeney and Ruzicka, 2004). Such large uncertainties directly reflect the variability of diffusion data. Alternatively, from this variability results a compensation rule, $\log D_0 = a + bE$ (diffusion coefficients are written $D = D_0 \exp(-E/RT)$). We test a new geospeemetry approach, based on this rule, on cooling of chondrules in chondrites, Sahara-97210 LL 3.2 and Wells LL 3.3. Greeney and Ruzicka (2004) matched Fe-Mg diffusion profiles in olivine from these chondrites with cooling rates between 200-6000 K/hr. In our geospeedometry model, the use of the compensation rule greatly reduces the uncertainties by avoiding the choice of one diffusion coefficient among many. The cooling rates we found are between 700-3600 K/hr for Sahara and 700-1600 K/hr for Wells. Finally, we discuss the influence of our analytical model parameters on our cooling rate estimates.

Key words: Compensation rule, Diffusion, Geochronology, Cooling rate, Meteorite
PACS: 66.30.-h, 91.35.Nm, 96.50.Mt

1 Introduction

Chondrites are the most abundant class of meteorites observed to fall on Earth. The name "chondrites" reflects that they usually contain large amounts (up to 80%) of small (millimeter-sized) spherules called chondrules. Their spherical shape shows evidence of solidification from liquid droplets in low gravity in the solar nebula. However their formation conditions and their significance are still unclear and a debated issue: being putative building blocks of planets it is not yet established whether they form prior, during or after accretion of planitesimals (Grossman, 1988). In other words the central question is wether the heating mechanism was an astrophysical or a planetary process. Cuzzi and Alexander (2006) proposed shock waves as a possible mechanism (see also, Desch, 2006) and outlined that cooling rates of chondrules may bring important constraints to this problem. It is therefore important to precisely determine (*i.e.*, with minimal error bars) these cooling rates.

Chondrules show a wide range of compositional and textural types depending upon their precursor and their thermal history. Their constituents are olivine, pyroxenes, Si and Al-rich glass, minor Na-K-Ca framework silicates, Fe-Ni alloy, sulfides and oxides. Olivine is here the first phase to nucleate from the

* Corresponding author
Email addresses: bejina@lmtg.obs-mip.fr (Frédéric Béjina),
vsautter@mnhn.fr (Violaine Sautter).

melt. It has long been argued that olivine speedometer, giving "absolute cooling rate", was reliable such that Fe-Mg zoning in olivine has been used in a variety of chondrites as a guide to cooling rate during chondrule crystallization. Unfortunately, most of the contributions using olivine speedometer are negligent (or at least optimistic) about the uncertainties of their cooling rate estimates. Obtained cooling rates range from 5 to 8400 K/hr (Desch and Connolly Jr., 2002; Greeney and Ruzicka, 2004), a scatter that reflects in part the uncertainties of diffusion data of a given element in a given mineral (here Fe-Mg in olivine) which varies as a function of experimental conditions (differences in olivine composition, fO_2, crystallographic direction etc.) Alternatively, estimates based on other approaches, such as textural observations compared with products from controlled cooling crystallization experiments or isotopic zoning (*e.g*, Yurimoto and Wasson, 2002; Tachibana et al., 2006), also bear large uncertainties. In this work, we test a new geospeedometry approach on relict olivine in type I chondrules from unequilibrated ordinary chondrite analysed by Greeney and Ruzicka (2004) [noted GR04]. Their cooling rate estimates vary from 200 to 6000 K/hr, a range probably larger than of most chondrules (see for example, Desch and Connolly Jr., 2002). Other independent estimates (Hewins et al., 2005, and references therein) favor lower cooling rates, from 10 to 1000 K/hr, during chondrule crystallization. Our approach based on the compensation rule (Jaoul and Sautter, 1999; Jaoul and Béjina, 2005) reduces significantly the uncertainties due to input diffusion parameters, and thus better constrains the thermal history during chondrule formation.

2 Presentation of the material

The samples we revisited here are relict olivines in chondrules from two ordinary LL-type chondrites, Sahara-97210 and Wells, recently studied by GR04 (Figs. 1 and 2 reproduce the concentration profiles of Fe, Mn and Ca they measured). The specimens contain highly magnesian olivine with initial composition Fo99. These are subhedral to euhedral olivine relict grains with [Ca] = 0.31 at% in Sahara and 0.29% in Wells. They are surrounded with epitaxial Fe-rich overgrowths containing a fair amount of Mn (Fo73 with [Mn] = 0.35% in Sahara, Fo70 with [Mn] = 0.33% in Wells). These relict olivines more likely crystallized as isolated grains outside the chondrule in the gas of the solar nebula whilst ferrous overgrowth formed probably later during the chondrule formation. The liquidus temperature for these overgrowths has been estimated around 1950 K (Hewins, 1997). The boundary between relict olivine and overgrowth show marked zonation, interpreted as diffusion profiles (Figs. 1 and 2), providing a record of the cooling conditions prevailing during the initial stage of the chondrule formation from a peak temperature, T_0 = 1950 K. Among the diffusion profiles shown in Figs. 1 and 2, Fe and Mg, two major elements, show a 30% change in concentration during diffusion which probably occured via octahedral vacancies. These defects have a concentration proportional to fO_2. Mn and Ca are minor elements: Mn diffusing in the same direction as Fe is probably exchanging with Mg; Ca diffuses opposite to Fe accompanying Mg in its exchange with Fe. Taken together these coupled interdiffusion imply most likely the same main point defects, M1 and M2 vacancies (Ca can only occupy M2 sites). In such a chondrite, diffusion probably occured under reducing conditions, 2 log units below IW [GR04].

The boundary conditions of Sahara (Fig. 1) are rather simple with constant compositions in Fe, Mg, Ca and Mn at $x > 0$ and $x < 0$ on both sides of the interface ($x = 0$), with diffusion starting at $t = 0$ and $T_0 = 1950$ K. The interface between forsterite and overgrowth is locally straight and traverses were obtained perpendicular to it.

The boundary conditions of Wells (Fig. 2) are less clear because the olivine system was obviously opened between the overgrowth and the rest of the chondrule. Therefore the overgrowth cannot be considered as a semi-infinite medium. The external chondrule feeds the overgrowth with Fe and Ca, and Mn escapes from it. The diffusion profiles printed in the overgrowth are too long compared to its thickness and only Ca apparently shows a decoupled exchange between forsterite and overgrowth and between overgrowth and chondrule. It is therefore the only case where the overgrowth can be approximated as a semi-infinite source.

3 Diffusion modelling

In order to extract a cooling rate from a diffusion profile one has to solve Fick's second law linking concentration variations with the instantaneous change of the profile curvature. The solution, $C(x, t)$, is the integration of this partial differential equation over the time duration of efficient diffusion. The solutions are tied to the initial and boundary conditions specific to the rock under studied (see above). To simulate $C(x, t)$ of the studied profiles, two approaches, analytical and numerical, are possible. Analytical solutions are mathematical functions of temperature, grain size, cooling rate and diffusion parameters. As diffusion is temperature dependent and temperature

changes with time, one has to solve a non-isothermal diffusion problem. This is the so-called geospeedometry approach (Dodson, 1973; Lasaga, 1983; Dodson, 1986). Alternatively numerical approaches solve the diffusion equation with discrete time and space using finite-difference techniques and diffusion parameters that change continuously on cooling. GR04 used such a numerical approach based on a simple diffusion model involving exchange between two semi-infinite media. We chose an analytical approach with diffusion between two semi-infinite sources as well, in contact at $x = 0$ and with initial concentrations C_1 and C_2 respectively. We only consider 1-D diffusion along x perpendicular to the planar interface. On four of the concentration profiles (Figs. 1 and 2), we have drawn the horizontal asymptotic lines for $C(x \to -\infty) = C_1$ and $C(x \to +\infty) = C_2$, as well as the tangent to the S-shaped curve in the vicinity of the inflexion point. Assuming for simplicity a simple error-function shape for the profiles, the intersections of the tangent with the two asymptotic lines gives two points separated by $\Delta x = 3.544\sqrt{Dt}$ (the calculation is easily done knowing that $d\mathrm{erf(x)}/dx = (2/\sqrt{\pi})e^{-x^2}$), in the case of isothermal diffusion with D constant with time, hence a diffusion characteristic length:

$$x_c = 2\sqrt{Dt} = 0.564\Delta x. \tag{1}$$

3.1 Thermal history: solution of non isothermal diffusion

We consider, as in Lasaga's model (1983), a linar initial cooling rate:

$$T(t) = T_0 - s_{\mathrm{init}}t, \tag{2}$$

starting from the peak temperature, T_0, at time $t = 0$, and with s_{init} a constant initial cooling rate. As shown, for example, by Ganguly et al. (1994) this is

consistent with a total cooling history that slows down with time. In our case, a linear equation is sufficient because diffusion is only efficient at high temperature, *i.e.* at the very beginning of the cooling cycle.

The determination of cooling rates using an analytical approach (Dodson, 1973; Lasaga, 1983; Dodson, 1986; Jaoul and Sautter, 1999; Jaoul and Béjina, 2005) requires a constant diffusion coefficient. However, in a cooling system, diffusion becomes non-isothermal and strongly slows down with time. The evolution of the diffusion coefficient during temperature decrease is expressed:

$$D(T(t)) = D_0 \exp\left(-\frac{E}{RT(t)}\right), \tag{3}$$

where D is an interdiffusion coefficient, D_0 the preexponential factor, E the activation energy, R the gas constant and T the temperature in Kelvin. Combining Eqs. (2) and (3) and following Dodson (1973) and Lasaga (1983), one can easily express $D(T(t))$ as a function of a time constant, τ:

$$D(T(t)) = D(T_0) \exp\left(-\frac{t}{\tau}\right), \tag{4}$$

where $D(T_0)$ is the diffusion coefficient at temperature T_0 and,

$$\tau = \frac{RT_0^2}{Es_{\text{init}}}. \tag{5}$$

Thereby Fick's law with a time-dependent diffusion coefficient becomes a simple equation where only $D(T_0)$ intervenes.

3.2 Analytical solution to the diffusion equation

The equation of diffusion:

$$\frac{\partial C}{\partial t} = D(T_0)\exp\left(\frac{-t}{\tau}\right)\frac{\partial^2 C}{\partial x^2}, \tag{6}$$

can be rewritten:

$$\frac{\partial C}{\partial t'} = D(T_0)\frac{\partial^2 C}{\partial x^2}, \tag{7}$$

with $t' = \tau(1 - e^{-t/\tau})$ and, therefore, when $t \to \infty$, $t' \to \tau$. Diffusion occurs with a decreasing D for t varying from 0 to ∞ or, equivalently with constant $D(T_0)$ and t' stopping at $t' = \tau$. The solution to the diffusion equation, $C(x,t)$ with C_1 and C_2 the initial concentrations at $x < 0$ and $x > 0$ respectively and leading to profiles with a similar shapes as those measured by GR04 (Figs 1 and 2), is:

$$C(x,t') = \frac{C_1 + C_2}{2} + \frac{C_2 - C_1}{2}\mathrm{erf}\left(\frac{x}{2\sqrt{D(T_0)t'}}\right), \tag{8}$$

with a diffusion characteristic length (defined in all diffusion textbooks such that the argument of the erf function is equal to 1), $x_c = 2\sqrt{D(T_0)t'}$, *i.e.* after $t \to \infty$:

$$x_c = 2\sqrt{D(T_0)\tau}. \tag{9}$$

As shown in Figs 1 and 2, x_c can be directly measured on the diffusion profiles by measuring Δx (see Eq. (1) and Fig. 1A). Then, Eqs. (5) and (9) provide,

$\tau = x_c^2/4D(T_0)$, so that:

$$s_{\text{init}} = \frac{4D(T_0)RT_0^2}{Ex_c^2}. \tag{10}$$

This formula is equivalent to Ganguly et al.'s (1994) in which the authors expressed s as a function of the total length of the diffusion profile, X_T, and using the relation, $x_c = 8X_T$.

4 Choice of diffusion coefficient and compensation rule

One of the major difficulties in all geospeedometry models is the diffusion coefficient. In the case of divalent cation diffusion in olivine, experimental measurements of D spread over a wide range of values and this leads to uncertainties of several orders of magnitude on the determination of s (*e.g.,* Spear and Parrish, 1996). The choice of D is therefore of prime importance but can be cumbersome for a non-specialist in diffusion and point-defect chemistry. Putting experimental uncertainties aside, this variability of diffusion coefficients exists because D depends upon many parameters: the thermodynamic conditions (T, $f\mathrm{O}_2$, $p\mathrm{H}_2\mathrm{O}$, etc.) under which D is measured modify the point-defect population resulting in different values of (E, D_0) (and eventually lead to different diffusion regimes); crystallographic orientation, dislocation density, etc., also affect atomic diffusion. Among these various parameters, some can be controlled or measured while some dependencies are known but not always well quantified. Of course, there is also the inherent variability of the experimental approach since no measurement has an infinite precision.

When applying geospeedometry models the best scenario is when the ther-

modynamic and physical conditions of the process under study are perfectly known. Therefore one can either chose the proper D value accordingly or re-calculate D if all the above dependencies are known. But this is rarely the case. For example GR04 assume diffusion coefficients to be independent of Fe content and do not take the crystallographic orientation into consideration but only consider fO_2 dependency. Therefore one is left with large uncertainties in the estimation of cooling rates. The one attempt that has been made to solve this problem is the use of the compensation rule, also called the Meyer-Neldel rule (Jaoul and Sautter, 1999; Jaoul and Béjina, 2005). In the next section, we present in detail how we built our compensation rule, keeping in mind that it should remain a tool easy to use.

4.1 Diffusion data and compensation rule

The compensation rule is an empirical correlation observed for many thermally-activated processes and in particular atomic diffusion (*e.g.,* Poirier, 2000):

$$\log D_0 = a + bE. \tag{11}$$

From parameter b, the "isokinetic" temperature, T^*, can be calculated, representing the theoretical temperature at which all diffusion coefficients along this line are equal to D^* (Hart, 1981). Our purpose is not to find a physical meaning to this correlation (examples can be found in Limoge and Grandjean, 1997; Lasaga, 1998) but to use it as an empirical relation (such as the calibration of infra-red spectroscopy to measure OH concentration in minerals). Nevertheless, to be applicable the compensation rule has to reflect at least a common specificity of all the data, an hypothesis that is implicitly made

throughout the paper. This is why we only compare divalent cation diffusion data in olivine since they probably all diffuse via the same mechanism in all directions (maybe except for Ca that can only enter M2 sites in the olivine structure) as shown by theoretical calculations (*e.g.*, Walker et al., 2008).

In previous works (Jaoul and Sautter, 1999; Jaoul and Béjina, 2005), it has been proposed that this rule can be a tool for the "diffusion neophyte" to avoid the choice of (E, D_0) among sometimes many and therefore reduce the uncertainties on the determination of the cooling rate. This point is obvious when, as in (Jaoul and Béjina, 2005), E can be extracted directly from the rock under study. But in most cases a choice of D has to be made and it seems legitimate that the compensation rule reduces the uncertainties around the calculated cooling rate because it acts as a smoothing filter. As shown by Eq. (10), s is very sensitive to $D(T_0)$ and, because the compensation rule limits the range of D_0, it also reduces the possible values for $D(T_0)$ (the problem of uncertainties is discussed in §4.1.3).

4.1.1 The diffusion data

In this paper, we only chose divalent-cation diffusion data measured in Fe-bearing olivines from Fo86 to Fo92, a composition range close to the olivine composition found at the center of the compositional profiles measured by GR04. There is now a large number of 2+cation diffusion measurements in olivine and Table 1 lists the selected ones. Some were not selected because they were never published or if so, only in conference abstracts, or because the fO_2 conditions are unknown (Clark and Long, 1971; Misener, 1974). We also did not include the diffusion coefficient by Hier-Majumder et al. (2005)

because it was measured under very high fH_2O and it is therefore not relevant for this study.

All selected data presented in Table 1 are for $fO_2 = 10^{-12}$ atm. When measured at a different fO_2, (E, D_0) were recalculated for 10^{-12} atm. For all but Ca diffusion data, we applied a dependency $D \propto {fO_2}^n$ with $n = 1/5.5$ (Nakamura and Schmalzried, 1984; Hermeling and Schmalzried, 1984). Other authors have found slightly different values for n: $\sim 1/5.8$ (Buening and Buseck, 1973), $\sim 1/3.2$, $\sim 1/5$ and $\sim 1/4.5$ for Mg, Fe and Mn respectively (Jurewicz and Watson, 1988) (note that for Fe diffusion along the $\vec{a}$ axis, these authors found $n = -0.18$), 1/4.25 (Petry et al., 2004) and Dohmen et al. (2007) found n between 1/5 and 1/7 (these authors also found that at low temperature and/or $fO_2 < 10^{-15}$ atm, n becomes much smaller). For Ca diffusion, for which we only have 2 data sets available, we chose $n = 1/3.2$ (Coogan et al., 2005) whereas Jurewicz and Watson (1988) found $n \simeq 1/4.5$.

Diffusion of divalent cation in olivines also depends upon the Fe content of the sample. All the data in Table 1 were measured in olivines Fo86-Fo92 and no correction was applied because, for such a narrow range of composition, the effect is much smaller than the uncertainties around D. On the other hand, for the determination of the cooling rate, the correction will be necessary because the Fe content can be as high as Fo75 (see §5).

4.1.2 Building the compensation rule

The compensation rule (Fig. 3) was built using the data in Table 1 corrected for $fO_2 =$ OSI (Olivine-Silica-Metal Fe-O_2 gas, about 2 orders of magnitude below Iron-Wustite) in order to be compatible with GR04. According to Nitsan

(1974), the equilibrium of Fo90 with silica and iron (and O_2) can be written:

$$\ln(fO_2)^{\mathrm{OSI}}\ (\mathrm{atm}) = 10.70 - \frac{541\ (\mathrm{kJ/mol})}{RT}. \tag{12}$$

Using the fO_2 dependency as described above, (E, D_0) were calculated to $fO_2 = \mathrm{OSI}$ using the relations:

$$\log(D_0)^{\mathrm{OSI}} = \log D_0 + 3.03\ (\mathrm{cm^2/s}), \tag{13}$$
$$E^{\mathrm{OSI}} = E + 93.5\ (\mathrm{kJ/mol}), \tag{14}$$

for Fe, Mg, Mn and Ni diffusion, and for Ca:

$$\log(D_0)^{\mathrm{OSI}} = \log D_0 + 5.16\ (\mathrm{cm^2/s}), \tag{15}$$
$$E^{\mathrm{OSI}} = E + 159.3\ (\mathrm{kJ/mol}). \tag{16}$$

4.1.3 Fitting routines and errors

For the compensation rule to be reliable, great care has to be taken in the fitting procedure. Linear fitting of a cloud of data points is not as easy as one would like. Least-squares routines are the most common but this method is very sensitive to points lying outside the cloud. A number of so-called robust routines, less sensitive to isolated data, exists (Press et al., 1992). To fit the diffusion data we used a basic linear regression (which is more a calculation than a fitting process) and a robust method of absolute deviation minimization (Press et al., 1992). The results for both methods can be compared in Table 2.

An additional problem arises from the uncertainties around E and D_0. When looking at the literature, one finds several cases:

(1) references with no uncertainties (these tend to be less frequent),

(2) authors who give uncertainty only around E,

(3) fortunately, in recent publications, errors both around E and D_0 are now given,

(4) but error bars on fO_2 or composition dependency are still extremely rare.

The problem runs deeper because uncertainties are not evaluated by all authors in the same manner and, actually, there is no description on the determination of these uncertainties. Rarely did authors try to estimate the "true experimental" uncertainty around their data, equivalent to running the same exact experiment many times. This procedure, largely too time-consuming for diffusion studies, is the only way to obtain a dispersion of points representing the influence of all parameters on the results (from sample preparation to measurement precision). Many authors probably give as uncertainties around their D values the 1σ deviation of a fit of a concentration profile measurement, and most published uncertainties around E and D_0 are also 1σ deviation of the fit of Arrhenius plots (1σ only represent a 68% confidence interval). Usually, these data points are too few to be statistically representative and, in addition, most of the fits do not take error bars around the data into account. Finally, because of the lack of statistics in most experimental works, the distribution of the errors around each data point is unknown.

Since we cannot circumvent these problems, we adopted the following procedure:

- When uncertainties around E and D_0 are given in the original publications, we reported these values as is and considered them to be 1σ if not reported otherwise (Jaoul et al. (1995) give a 2σ error that we converted to 1σ for consistency with other data).
- When uncertainties around E and/or D_0 are missing we arbitrarily fixed

$\Delta E = 30$ kJ/mol and, because errors on E and D_0 are linked, we calculated ΔD_0 using a first estimate of the compensation rule that did not take error bars into account.

- We did not consider error bars around n, the fO_2 exponent.
- We compared a linear regression and a robust method, the latter using both a gaussian and a lorentzian distribution for the errors around the data points. We have no grounds to determine the exact nature of this error distribution. As can be found in most textbooks (*e.g.*, Press et al., 1992), a lorenztian distribution is probably closer to a real experimental uncertainty but leads to enormous error bars. But because error bars around D (and also around E and D_0) given by most authors probably correspond to 1σ deviation of a fit, this false error distribution is gaussian. We adopted this latter option.

4.1.4 The compensation rule

Data from Table 1 were recalculated for $fO_2 = \text{OSI}$ as described in §4.1.2 and plotted in Fig. 3. Results from the different fits are given in Table 2 and as can be seen on Fig. 3 fits using either methods are extremely close to each other (but not the uncertainties!) We therefore use the fitting parameters obtained from our robust fit and gaussian error distribution as explained previously, to determine the following compensation rule:

$$\log(D_0) = -9.9895 + 0.02701\frac{E}{RT}, \tag{17}$$

with D_0 in cm^2/s and E in kJ/mol, for Fe, Mg, Mn and Ni diffusion. This correlation for divalent-cation diffusion (except Ca) in olivine was first proposed by Hart (1981) and then by Jaoul and Sautter (1999) but without paying

much attention to the influence of fO_2 on D_0. Here, the compensation rule is given for $fO_2 = \mathrm{OSI}$ and accounts for the anisotropy of diffusion. The isotemperature calculated from the slope of the fit is $T^* = 1934$ K, whereas Hart (1981) found $T^* = 1633$ K and Jaoul and Sautter (1999), $T^* = 1775$ K.

For calcium, we obtain (D_0 in cm^2/s and E in kJ/mol):

$$\log(D_0) = -20.3657 + 0.05339\frac{E}{RT}, \tag{18}$$

This gives, $T^* = 978$ K, a much lower value than for the other 2+cations, but the lack of diffusion data makes this relation very unreliable.

5 Results and cooling rates

In the present section, we describe our determination of the cooling rates of the two chondrites, Sahara and Wells, previously studied by GR04. We did not consider here the results obtained using the Ca concentration profiles because (1) there is not enough diffusion data and the existing ones are clustered around similar (E, D_0) values to fit a reliable compensation rule and (2) the effect of composition on Ca diffusion is still very poorly known (these results are nevertheless listed in Table 3). Therefore, from now on, the term divalent-cation diffusion describes only Fe, Mg, Mn and Ni diffusion.

Eq. (10) shows that s can be calculated if E, T_0 and x_c are known, x_c being directly measured on the concentration profiles (see §3). As recalled previously, GR04 chose $T_0 = 1950$ K and the diffusion coefficients of Jurewicz and Watson (1988) and Chakraborty (1997) without taking into account the crystallographic orientation or the dependency with Fe content. For $fO_2 = \mathrm{OSI}$,

they calculated a cooling rate ranging from 340 to 8380 K/hr.

In Table 3 we present our results using the same $T_0 = 1950$ K as GR04. The listed values for $D(T_0)$, calculated as described in the caption of Table 3, are not corrected for Fe composition but this correction is made when calculating s for each x_c according to the mid-profile Fe composition. This correction is such that $D \propto 10^{3X_{\mathrm{Fe}}}$, an average value of experimental measurements of the influence of Fe composition on D (Nakamura and Schmalzried, 1984; Jaoul et al., 1995; Chakraborty, 1997; Dohmen et al., 2007). As one can see, the range of $D(T_0)$ is very narrow, for two reasons: (1) as we said previously, using the compensation law to determine D_0 knowing E (or vice-versa) is equivalent to applying a smoothing function and, (2), most importantly, $T^* = 1934$ K, the temperature at which all D values are equal to D^*, is very close to T_0. As a comparison, calculated values of $D(T_0)$ using the experimental values of (E, D_0) span over three orders of magnitude.

The range of cooling rates, calculated using Eq. (10), is much narrower than GR04's. For Sahara we found from about 700 K/hr to 1520 K/hr (x_c = 5.5 μm), 1580 K/hr to 3360 K/hr (x_c = 5.4 μm), 1170 K/hr to 2500 K/hr ($x_c = 5.1$ μm) and, for Wells, 750 K/hr to 1600 K/hr ($x_c = 4.5$ μm).

6 Error analysis and sensitivity of s_{init} to the model's parameters

The initial cooling rate, s_{init}, is given by Eq. (10). It depends on x_c, T_0, and the diffusion parameters E and D_0, or a, b and E if the compensation rule is taken into account.

Sensitivity to $\mathbf{x_c}$ is given by:

$$\partial \log s_{\text{init}} = -\frac{2}{2.303}\frac{\partial x_c}{x_c}, \tag{19}$$

so that an error of +10% on x_c induces a change of -0.09 on $\log s_{\text{init}}$, *i.e.*, an underestimate of 23% on s_{init}, which cannot be neglected.

Sensitivity to $\mathbf{T_0}$ is:

$$\partial \log s_{\text{init}} = -\frac{2}{2.303}\left(\frac{E}{RT_0}+2\right)\frac{\partial T_0}{T_0}. \tag{20}$$

With $E = 300$ kJ/mol and $T_0 = 1950$ K as it is approximately for chondrites Sahara and Wells, s_{init} decreases by 1 order of magnitude if T_0 is lowered by 200 K. This is the main source of uncertainty on s_{init}. The present estimate is in contradiction with that of GR04 when they compare the two situations, $T_0 = 1950$ K and $T_0 = 1500$ K, for which they surprisingly indicate very similar s_{init} values. In fact, T_0 must be known from other independent means than the present diffusion profiles.

Sensitivity to $\mathbf{D_0}$ and E: These two diffusion parameters have a strong influence on the precision of the cooling rate:

$$\partial \log s_{\text{init}} = \partial \log D_0 - \frac{1}{2.303}\left(\frac{1}{RT_0}+\frac{1}{E}\right)\partial E, \tag{21}$$

and the uncertainty Δ, *i.e.*, the maximum absolute value of the error ∂ in the approximation of independent parameters, is:

$$\Delta \log s_{\text{init}} = \Delta \log D_0 + \frac{1}{2.303}\left(\frac{1}{RT_0}+\frac{1}{E}\right)\Delta E. \tag{22}$$

In the present case, ignoring the existence of the compensation rule and considering, for example, $\Delta \log D_0 \simeq 1$ and $\Delta E \simeq 30$ kJ/mol (one standard deviation only) around $E = 300$ kJ/mol, $T_0 = 1950$ K, one finds $\Delta \log s_{\text{init}} = 1.85$ meaning that s_{init} is known within $s_{\text{init}} \times 70$ and $s_{\text{init}}/70$.

This huge uncertainty was not considered by GR04 who only bracket $s_{\rm init}$ by simply evaluating the quality of their fits to the data, not considering the uncertainties ΔE and $\Delta \log D_0$, and even less a different set of (E, D_0).

Sensitivity to a, b, and E: We now consider the use of the compensation rule and the differentiation of Eqs. (10) and (11) yields:

$$\partial \log s_{\rm init} = \partial a + E\partial b + \left(b - \frac{1}{2.303RT_0} - \frac{1}{2.303E}\right)\partial E, \tag{23}$$

with the uncertainty:

$$\Delta \log s_{\rm init} = \Delta a + E\Delta b + \left|b - \frac{1}{2.303RT_0} - \frac{1}{2.303E}\right|\Delta E. \tag{24}$$

This first two terms correspond to the absolute calibration of the compensation tool. The last term intervenes when comparing profiles and is small because terms between parentheses [Eq. (24)] compensate. Remembering that $b = 1/2.303RT^\star$, this term becomes very small when T_0 is close to $T^\star$. In the present case with $T_0 \simeq T^\star$, we take full advantage of the compensation correlation with $1/2.303RT_0 = 0.02678$ mol/kJ and $b = 0.02701$ mol/kJ.

Sensitivity to $\mathbf{fO_2}$: As $s_{\rm init} \propto D_0 \propto {fO_2}^{1/5.5}$, its value is modified by one order of magnitude if fO_2 is changed by 5.5 orders of magnitude. Thus, around the conditions $\log fO_2 \simeq {\rm OSI} \pm 2$ log units, the uncertainty on fO_2 does not change the order of magnitude of $s_{\rm init}$.

7 Conclusion

Altogether, data obtained on Sahara and Wells chondrules by GR04 suggest typical cooling rates of 200-6000 K/hr. Using our geospeedometer based on the compensation law on the same samples significantly narrows this range of

values down to 700-3600 K/hr for Sahara and 700-1600 K/hr for Wells. The advantage of using the compensation rule is thus manyfold. It reduces uncertainties on cooling rate values because error on D_0 and E are no longer added but instead efficiently compensate each other. The rule gives more precise results when applied to a mineral such as olivine for which avalaible experimental data are numerous, thus allowing a statistical overview with associated standard deviations. It avoids the choice of one particular diffusion coefficient among many or of the diffusion direction (the error analysis presented in §6 accounts for these variabilities.) For instance GR04 have no real justification for their choice of Jurewicz and Watson (1988)'s data and of the particular $\vec{c}$ crystallographic direction. Without judging the quality of these data (Jurewicz and Watson, 1988), they were nevertheless obtained over a narrow range of T and are therefore difficult to extrapolate far ouside this range. Even if the compensation rule cannot give an exact and precise cooling rate (an intrinsic limitation of geospeedometry) it nevertheless narrows considerably the range of possible values, in particular the fastest ones. Generally, extracting a cooling rate from such compositional profiles would necessitate the use of a multicomponent approach, or at least an effective binary diffusion model (*e.g.*, Ganguly et al., 1996). In the cases presented here, Ca and Mn concentrations are low enough so that the use of a more complex model is not necessary and would give results well within our range of possible cooling rates, and therefore would change the overall conclusion.

Acknowledgements

This work was originally started by Olivier Jaoul but he didn't have the chance to complete it. We would like to thank M. Ito and J. Ganguly for their constructive reviews.

References

Buening, D. K., Buseck, P. R., 1973. Fe-Mg lattice diffusion in olivine. J. Geophys. Res. 78 (29), 6852–6862.

Chakraborty, S., 1997. Rates and mechanisms of Fe-Mg interdiffusion in olivine at 980°-1300°C. J. Geophys. Res. 102 (B6), 12317–12331.

Chakraborty, S., Farver, J. R., Yund, R. A., Rubie, D. C., 1994. Mg tracer diffusion in synthetic forsterite and San Carlos olivine as a function of P, T and fO_2. Phys. Chem. Minerals 21, 489–500.

Clark, A. M., Long, J. V. P., 1971. The anisotropic diffusion of nickel in olivine. In: Sherwood, J. N., Chadwick, A. V., Muir, W. M., Swinton, F. L. (Eds.), Diffusion Processes. Vol. 2. Gordon and Breach Science Publishers, London, pp. 511–521.

Coogan, L. A., Hain, A., Stahl, S., Chakraborty, S., 2005. Experimental determination of the diffusion coefficient for calcium in olivine between 900°C and 1500°C. Geochim. Cosmochim. Acta 69 (14), 3683–3694.

Cuzzi, J. N., Alexander, C. M. O'D., 2006. Chondrule formation in particle-rich nebular regions at least hundreds of kilometres across. Nature 441, 483–485.

Desch, S., 2006. Meteoritics: How to make a chondrule. Nature 441, 416–417.

Desch, S. J., Connolly Jr., H. C., 2002. A model for the thermal processing of

particles in solar nebula shocks: application to cooling rates of chondrules. Meteorit. Planet. Sci. 37, 183–208.

Dodson, M. H., 1973. Closure temperature in cooling geochronological and petrological systems. Contrib. Mineral. Petrol. 40, 259–274.

Dodson, M. H., 1986. Closure profiles in cooling systems. In: Materials Science Forum. Vol. 7. Trans Tech Publications Ltd., Switzerland, pp. 145–154.

Dohmen, R., Becker, H.-W., Chakraborty, S., 2007. Fe-Mg diffuson in olivine I: experimental determination between 700 and 1,200∘C as a function of composition, crystal orientation and oxygen fugacity. Phys. Chem. Minerals 6 (34), doi:10.1007/s00269–007–0157–7.

Dohmen, R., Chakraborty, S., 2007. Fe-Mg diffuson in olivine II: point defect chemistry, change of diffusion mechanisms and a model for calculation of diffusion coefficients in natural olivine. Phys. Chem. Minerals 6 (34), doi:10.1007/s00269–007–0158–6.

Ganguly, J., 2002. Diffusion kinetics in minerals: principles and applications to tectono-metamorphic processes. In: Gramaccioli, C. (Ed.), EMU Notes in Mineralogy. Vol. 4. Etvs University Press, Budapest, Ch. 10, pp. 271–309.

Ganguly, J., Yang, H., Ghose, S., 1994. Thermal history of mesosiderites: Quantitative constraints from compositional zoning and Fe-Mg ordering in orthopyroxenes. Geochim Cosmochim Acta 58, 2711–2723.

Ganguly, J., Chakraborty, S., Sharp, T. G., Rumble, D., 1996. Constraint on the time scale of biotite-grade metamorphism during Acadian orogeny from a natural garnet-garnet diffusion couple. Am. Mineral. 81, 1208–1216.

Greeney, S., Ruzicka, A., 2004. Relict forsterite in chondrules: implications for cooling rates. Lunar Planet. Sci. XXXV, abstract # 1246.

Grossman, J. N., 1988. Formation of chondrules. In: Kerridge, J. F., Matthews, M. S. (Eds.), Meteorites and the Early Solar System. Univ. of Arizona Press,

Tucson, pp. 680–696.

Hart, S. R., 1981. Diffusion compensation in natural silicates. Geochim. Cosmochim. Acta 45, 279–291.

Hermeling, J., Schmalzried, H., 1984. Tracerdiffusion of the Fe-cations in olivine $(Fe_xMg_1 - x)_2SiO_4$ (III). Phys. Chem. Minerals 11, 161–166.

Hewins, R., 1997. Chondrules. Ann. Rev. Earth Planet. Sci. 25, 61–83.

Hewins, R., Connolly Jr., H., Lofgren, G., Libourel, G., 2005. Experimental constraints on chondrule formation. In: Krot, A., Scott, E., Reipurth, B. (Eds.), Chondrites and the Protoplanetary Disk. Vol. 341 of Astronomical Society of the Pacific Conference Series. pp. 286–317.

Hier-Majumder, S., Anderson, I. M., Kohlstedt, D. L., 2005. Influence of protons on Fe/Mg interdiffusion in olivine. J. Geophys. Res. 110, B02202doi: 10.1029/2004jb003292.

Jaoul, O., Béjina, F., 2005. Empirical determination of diffusion coefficients and geospeedometry. Geochim. Cosmochim. Acta 69 (4), 1027–1040.

Jaoul, O., Bertran-Alvarez, Y., Liebermann, R. C., Price, G. D., 1995. Fe–Mg interdiffusion in olivine up to 9 GPa at $T = 600$–$900°C$; experimental data and comparison with defect calculations. Phys. Earth Planet. Inter. 89, 199–218.

Jaoul, O., Sautter, V., 1999. A new approach to geospeedometry based on the 'compensation law'. Phys. Earth Planet. Inter. 110, 95–114.

Jurewicz, A. J. G., Watson, E. B., 1988. Cations in olivine, Part 2: Diffusion in olivine xenocrysts, with applications to petrology and mineral physics. Contrib. Mineral. Petrol. 99, 186–201.

Lasaga, A. C., 1983. Geospeedometry: An extension of geothermometry. In: Saxena, S. K. (Ed.), Kinetics and Equilibrium in Mineral Reactions. No. 3 in Advances in Physical Geochemistry. Springer-Verlag, New York, Ch. 3,

pp. 81–114.

Lasaga, A., 1998. Kinetic Theory in the Earth Sciences. Princeton Series in Geochemistry. Princeton University Press, pp. 728.

Limoge, Y., Grandjean, A., 1997. On the Correlations between Activation Enhalpies and Entropies of Activated Processes in the Solid State. Defect Diff. Forum 143-147, 747–752

Meissner, E., Sharp, T. G., Chakraborty, S., 1998. Quantitative measurement of short compositional profiles using analytical transmission electron microscopy. Amer. Mineral., 546–552.

Misener, D. J., 1974. Cationic diffusion in olivine to 1400°C and 35 kbar. In: Hofmann, A. W., Giletti, B. J., Yoder, Jr., H. S., Yund, R. A. (Eds.), Geochemical Transport and Kinetics. Carnegie Institution of Washington, pp. 117–129.

Nakamura, A., Schmalzried, H., 1984. On the Fe^{2+}-Mg^{2+} interdiffusion in olivine (II). Berischte der Bunsen Gesellschaft-Physical Chemistry-Chemical Physics 88, 140–145.

Nitsan, U., 1974. Stability field of olivine with respect to oxidation and reduction. J. Geophys. Res. 79 (5), 706–711.

Petry, C., Chakraborty, S., Palme, H., 2004. Experimental determination of ni diffusion coefficients in olivine and their dependence on temperature, composition, oxygen fugacity, and crystallographic orientation. Geochim. Cosmochim. Acta 68 (20), 4179–4188.

Poirier, J.-P., 2000. Introduction to the Physics of the Earth's Interior, 2nd Edition. Cambridge University Press, Cambridge, location: Biblio perso.

Press, W. H., Teukolsky, S. A., Vetterling, W. T., Flannery, B. P., 1992. Numerical Recipies in C: The Art of Scientific Computing, 2nd Edition. Cambridge University Press, Cambridge.

Spear, F. S., Parrish, R. R., 1996. Petrology and cooling rates of the Valhalla complex, British Columbia, Canada. J. Petrology 37 (4), 733–765.

Tachibana, S., Nagahara, H., Mizuno, K., 2006. Constraints on Cooling Rates of Chondrule from Metal-Troilite Assemblages. Lunar Planet. Sci. XXXVII, abstract # 2263.

Walker, A. M., Woodley, S. M., Slater, B., Wright, K., 2007. A computational study of magnesium points defects and diffusion in forsterite. Phys. Earth Planet. Inter., this issue.

Yurimoto, H., Wasson, J. T., 2002. Extremely rapid cooling of a carbonaceous-chondrite chondrule containing very ^{16}O-rich olivine and a ^{26}Mg-excess. Geochim. Cosmochim. Acta 66, 4355–4363.

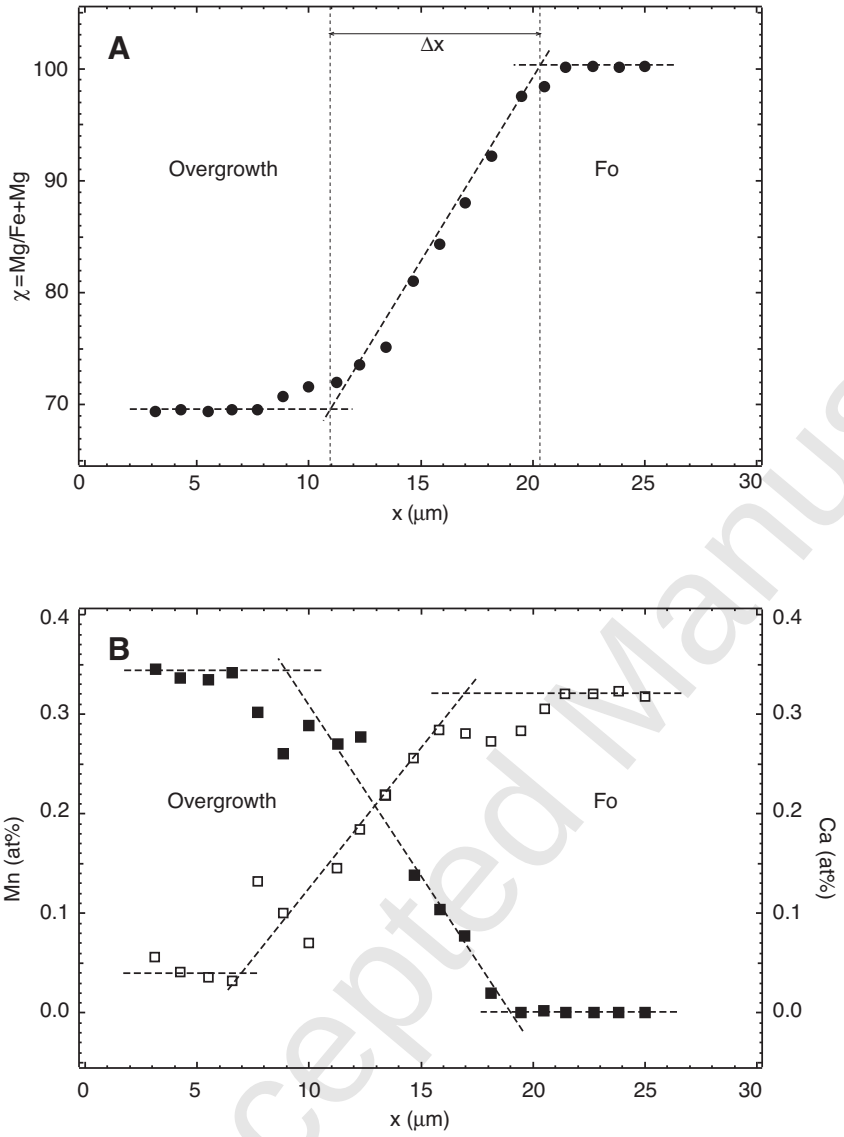

Fig. 1. Sahara-97210 LL3.2 chondrite (modified after Greeney and Ruzicka (2004)). (**A**) Fe-Mg and (**B**) Mn-Mg (black squares) and Ca-Fe (empty squares) zonations between the relict forsterite (on the right-hand side of the profiles) and the olivine overgrowth (left side). For each profile, Δx [Eq. (1)] is the distance between intersection points of the asymptotic lines to the tails of the profiles and the tangent of the S-shaped curve near the interface of exchanging minerals. The value of Δx allows to determine the diffusion characteristic length using Eq. (9).

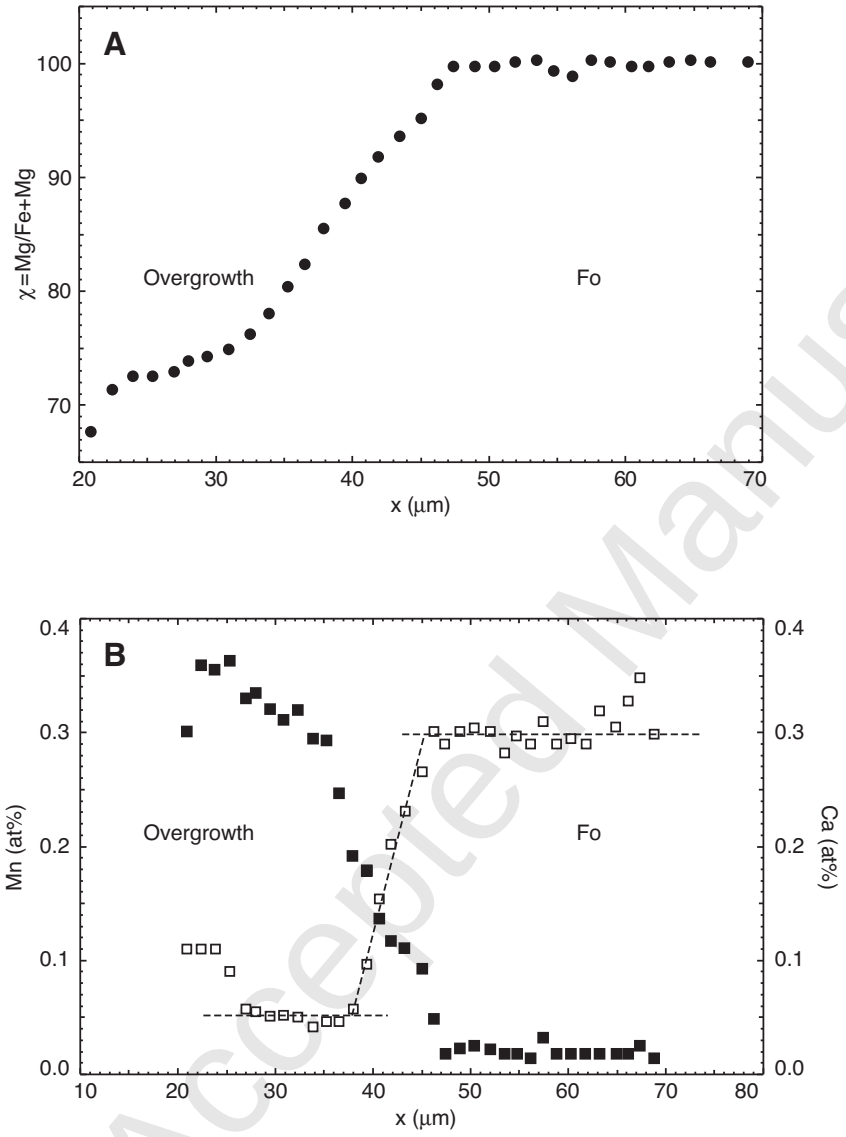

Fig. 2. Wells LL 3.3 chondrite (modified after Greeney and Ruzicka (2004)). (**A**) Fe-Mg and (**B**) Mn-Mg (black squares) and Ca-Fe (empty squares) zonations between the relict forsterite (on the right-hand side of the profiles) and the olivine overgrowth (left side).

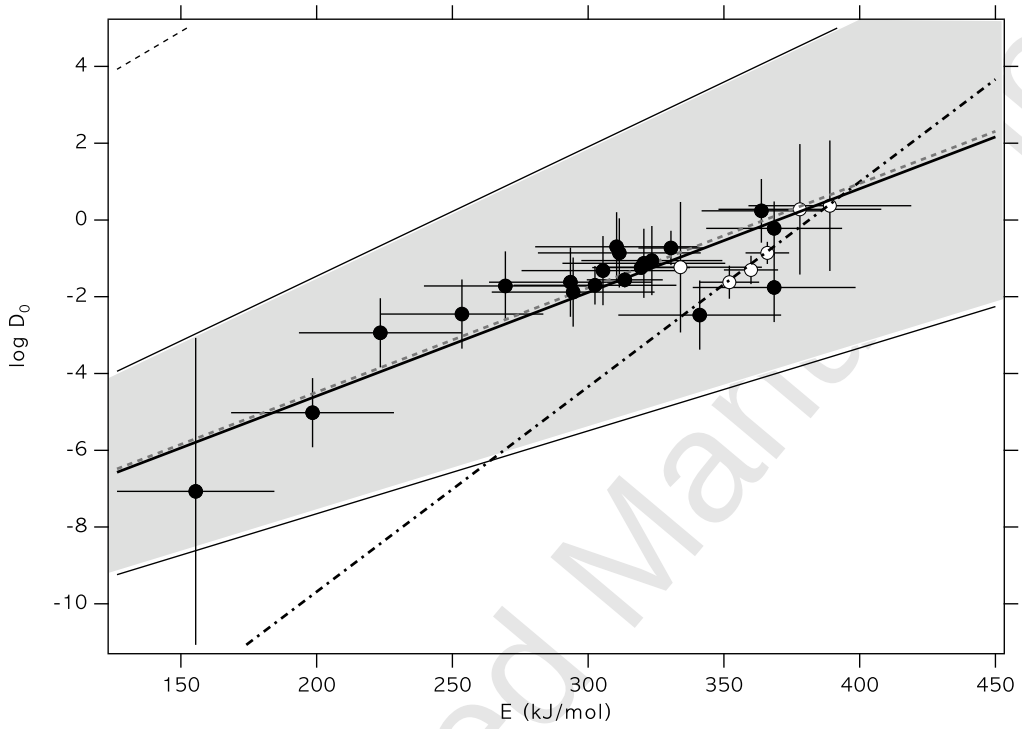

Fig. 3. The compensation rule for divalent cation diffusion measured in olivine Fo86 to Fo94 and recalculated at fO_2 = OSI. D_0 is in cm^2/s. White circles are Ca diffusion data, others are black dots. The black full lines are for the fit (except Ca data) obtained by our robust routine with a gaussian error distribution and its limits are shown by the grey area. Dashed grey lines are for a lorentzian error distribution which, by its nature, leads to a huge uncertainty (only the upper boundary is visible). The dot-dashed line is the fit to Ca diffusion only (gaussian error distribution) and, because of the very small number of data and the cluttering around the same (E, D_0) values, has uncertainties too large to show on this diagram.

Table 1

Divalent cation diffusion in olivine Fo86 to Fo94 at $fO_2 = 10^{-12}$ atm. Data obtained at known fO_2 other than 10^{-12} atm were recalculated as described in the text. Olivine crystallographic axes refer to the Pbnm space group.

(#) Refs.	Experiments	E (kJ/mol)	$\log D_0$ (cm^2/s)	Comments
(1) Buening and Buseck (1973)	Fe-Mg in Fo87	264	-1.54	$\vec{a}$, $T > 1125°C$
(2)		244	-1.72	$\vec{c}$, id.
(3)		176	-4.85	$\vec{a}$, $T < 1125°C$
(4)		160	-5.58	$\vec{b}$, id.
(5)		130	-6.07	$\vec{c}$, id.
(6) Nakamura and Schmalzried (1984)	Fe-Mg in Fo90	200	-4.65	polycrystal
(7) Jurewicz and Watson (1988)	Fe in Fo90	217	-3.73	$\vec{a}$, Inconsist.
(8)		105	-8.05	$\vec{b}$, id.
(9)		209	-4.73	$\vec{c}$, id.
(10) Jurewicz and Watson (1988)	Mn in Fo90	227	-4.16†	$\vec{a}$
(11)		212	-4.35	$\vec{b}$
(12)		218	-3.89	$\vec{c}$
(13) Jaoul et al. (1995)	Fe-Mg in Fo90	62 ± 29*	-10.10 ± 4.00*	$\vec{b}$, HP, Fe capsules
(14) Chakraborty et al. (1994)	Mg in Fo92	275 ± 25	-3.25 ± 0.90	$\vec{c}$
(15) Chakraborty (1997)	Fe-Mg in Fo86	226 ± 18	-4.27 ± 0.10	$\vec{c}$
(16) Meissner et al. (1998)[b]	Fe-Mg in Fo86	270 ± 22	-2.89 ± 0.83	$\vec{c}$
(17) Petry et al. (2004)[a]	Fe-Mg in Fo90	237 ± 12	-3.76 ± 0.45	$\vec{c}$
(18) Petry et al. (2004)	Ni in Fo90	220 ± 14	-4.59 ± 0.20	$\vec{c}$
(19) Petry et al. (2004)[a]	Mn in Fo90	230 ± 26	-4.09 ± 0.90	$\vec{c}$
(20) Dohmen and Chakraborty (2007)	Fe-Mg in Fo90	201	-4.91	$\vec{c}$
(21) Jurewicz and Watson (1988)	Ca in Fo90	230	-4.28	$\vec{a}$
(22)		219	-4.36	$\vec{b}$
(23)		175	-5.88	$\vec{c}$
(24) Coogan et al. (2005)	Ca in Fo92	193 ± 11	-6.78 ± 0.43	$\vec{a}$
(25)		201 ± 10	-6.46 ± 0.37	$\vec{b}$
(26)		207 ± 8	-6.02 ± 0.29	$\vec{c}$

([a])Recalculated from original data table; ([b]) Estimated from original Arrhenius plot;

* $\pm 2\sigma$.

Table 2

Parameters a (such that D is in cm^2/s) and b (in mol/kJ) of the compensation rule for diffusion data listed in Table 1 and corrected for $fO_2 = OSI$. All fits take error bars into consideration.

Linear regression						
	$a \pm 1\sigma$		$(b \pm 1\sigma) \times 10^2$		r	
Fe, Mg, Mn, Ni	-9.9329 ± 1.9582		2.7140 ± 0.6134		0.8750	
Ca	-21.0203 ± 27.7924		5.5177 ± 4.2412		0.8412	
Robust fit						
	a	b	$a_{\min}$	$a_{\max}$	$b_{\min}$	$b_{\max}$
	Gaussian distribution					
Fe, Mg, Mn, Ni	-9.9895	0.02701	-11.9760	-8.2056	0.02160	0.03371
Ca	-20.3657	0.05339	-63.9288	-9.2863	0.02251	0.1716
	Lorentzian distribution					
Fe, Mg, Mn, Ni	-9.9224	0.02718	-14.6346	-1.3469	7×10^{-5}	0.0417
Ca	-22.0115	0.05791	-68.7632	-1.4461	8×10^{-4}	0.1921

Table 3

Cooling rates s for selected diffusion data calculated for x_c = 5.5, 5.4, 5.1 and 4.5 μm using Eq. (10). $D(T_0)$ is determined using experimental E values corrected at fO_2 = OSI and corresponding D_0 calculated with the compensation rule. Estimates of s include a correction for the dependence of D with Fe content (estimated at mid-distance in the original concentration profiles of Greeney and Ruzicka (2004).)

Ref.(#)	$D(T_0)$ (cm^2/s)	s (K/hr)			
			Sahara		Wells
		5.5 μm (Fo85)	5.4 μm (Fo74)	5.1 μm (Fo80)	4.5 μm (Fo90)
Fe, Mg, Mn, Ni diffusion					
Buening and Buseck (1)	1.24×10^{-10}	713	1582	1172	755
(2)	1.22×10^{-10}	760	1686	1249	804
(3)	1.18×10^{-10}	927	2057	1524	981
(4)	1.17×10^{-10}	978	2169	1606	1034
(5)	1.15×10^{-10}	1092	2423	1794	1155
Nakamura and Schmalzried (6)	1.19×10^{-10}	862	1912	1416	912
Jurewicz and Watson (7)	1.20×10^{-10}	822	1823	1350	869
(8)	1.13×10^{-10}	1214	2693	1995	1284
(9)	1.20×10^{-10}	840	1864	1380	889
(10)	1.21×10^{-10}	800	1775	1315	846
(11)	1.20×10^{-10}	833	1848	1369	881
(12)	1.20×10^{-10}	820	1818	1347	867
Jaoul et al. (13)	1.11×10^{-10}	1516	3363	2491	1604
Chakraborty et al. (14)	1.24×10^{-10}	713	1582	1172	755
Chakraborty (15)	1.21×10^{-10}	803	1780	1318	849
Meissner et al. (16)	1.23×10^{-10}	721	1599	1184	762
Petry et al. (17)	1.20×10^{-10}	815	1808	1340	862
(18)	1.21×10^{-10}	794	1762	1305	840
(19)	1.21×10^{-10}	780	1730	1282	825
Dohmen and Chakraborty (20)	1.20×10^{-10}	815	1808	1340	862
Ca diffusion					
Jurewicz and Watson (21)	9.65×10^{-11}		387		558
(22)	4.92×10^{-11}		203		292
(23)	3.32×10^{-12}		15		22
Coogan et al. (24)	1.00×10^{-11}		44		64
(25)	1.63×10^{-11}		71		102
(26)	2.36×10^{-11}		101		145